FORCED CONVECTIVE HEAT TRANSFER IN NOVEL STRUCTURED PACKED BEDS OF PARTICLES

J. Yang, J.Wang, S.S. Bu, M. Zeng and Q.W. Wang *
*Author for correspondence
Key Laboratory of Thermal Science and Engineering of MOE,
Xi'an Jiaotong University,
Xi'an, Shaanxi, 710049, P.R. China,
E-mail: wangqw@mail.xjtu.edu.cn

ABSTRACT

Randomly packed beds are widely used in a variety of industries, because of their low cost and ease of use compared with other packing methods. However, the pressure drops in such packed beds are usually much higher than those in other packings, and the overall heat transfer performances may be greatly lowered. In order to reduce the pressure drops and improve the overall heat transfer performances of packed beds, structured packings are considered to be promising choices. In this paper, some of our recent contributions on the hydrodynamic and heat transfer characteristics in some novel structured packed beds are introduced, where the effects of packing form and particle shape are carefully investigated, and the numerical and experimental results are also compared in detail. Firstly, it is found that, with proper selection of packing form and particle shape, the pressure drops in the structured packed beds can be greatly reduced and the overall heat transfer performances will be improved. The traditional correlations of flow and heat transfer extracted from random packings are found to overpredict the pressure drops and Nusselt numbers for all the structured packings, and some modified correlations are obtained. Secondly, it is revealed that, both the effects of packing form and particle shape are significant on the flow and heat transfer in structured packed beds. With the same particle shape (sphere), the overall heat transfer efficiency of SC packing is the highest. With the same packing form, such as FCC or SC packings, the overall heat transfer performance of ellipsoidal particle model is better. Furthermore, with the same particle shape and packing form, such as BCC packing with spheres, the overall heat transfer efficiency of uniform packing is higher than that of non-uniform packing. [*Keyords:* Structured packing; Ellipsoidal particle; CFD, Experimental analysis]

NOMENCLATURE

a	[m]	Length of packed cell
a_1, a_2	[-]	Model constants in Nusselt number correlation
A	[m^2]	Area
b	[m]	Width of packed cell
c	[m]	Height of packed cell
c_1, c_2	[-]	Model constants in friction factor correlation
c_F	[-]	Forchheimer coefficient
c_p	[J/kg K]	Specific heat at constant pressure
d_h	[m]	Pore scale hydraulic diameter
d_p	[m]	Equivalent particle diameter
f	[-]	Friction factor
h_{sf}	[W/m^{2}K]	Heat transfer coefficient of particle to fluid
H	[m]	Height of computational domain or test packed bed
K	[m^2]	Permeability
L	[m]	Total length of computational domain or test packed bed
L_1	[m]	Length of inlet block for simulation
L_2	[m]	Length of packed channel for simulation
L_3	[m]	Length of outlet block for simulation
n	[-]	Model constant in Nusselt number correlation
N	[-]	Ratio of channel height to particle diameter
Nu_{sf}	[-]	Nusselt number of particle to fluid
p	[Pa]	Pressure
Pr	[-]	Prandtl number
Re	[-]	Reynolds number
T	[K]	Temperature
u	[m/s]	Velocity in x direction
V	[m^3]	Volume
$\vec{V}_D$	[m/s]	Darcy velocity vector
W	[m]	Width of computational domain or test packed bed
x, y, z	[m]	Coordinate directions

Special characters

γ	[W/m^{2}KPa]	Overall heat transfer efficiency for simulation
γ'	[W/m^{3}KPa]	Overall heat transfer efficiency for experiment
μ	[kg/ms]	Dynamic viscosity
ρ	[kg/m^3]	Density
ϕ	[-]	Porosity

Subscripts

$cell$	[-]	Value obtained in packed cell
exp	[-]	Value obtained by experiments
f	[-]	Fluid
in	[-]	Inlet section of packed cell
out	[-]	Outlet section of packed cell
p	[-]	Particle or packed bed
0	[-]	Inlet section of packed channel

INTRODUCTION

Packed beds, due to their high surface area-to-volume ratio, are widely used in a variety of industries, such as catalytic reactors, absorption towers, packed bed regenerators, high temperature gas-cooled nuclear reactors and heat accumulators, etc.

In the past decades, the flow and heat transfer in the packed beds, including random and structured packings, were extensively investigated by lots of researches. For example, for random packing, Carpinlioglu and Ozahi [1] have experimentally studied the pressure drop characteristics of a variety of randomly packed beds in turbulent flow of air. The measured pressure drops were compared with the well-known Ergun's equation [2] and the deviations were within an acceptable error margin. A simplified correlation for the measured pressure drop was obtained and it was observed to be correlated in terms of particle sphericity, porosity and Reynolds number. Lanfrey et al. [3] recently have developed a theoretical model for the tortuosity of fixed bed randomly packed with identical particles. They found that, the tortuosity was proportional to a packing structure factor, which could well capture the balancing effect between porosity and particle sphericity. A comparison between the performance in flow and heat transfer estimation of different turbulence models in a randomly packed bed were also performed by Guardo et al. [4]. It was found that, the Spalart–Allmaras turbulence model was better than the two-equation RANS model and the computational results of pressure drop and heat transfer coefficient could fit well with the traditional empirical correlations (Ergun' equation [2] and Wakao's equation [5]). Some other recent studies for random packing were also reported by Guo and Dai [6] and Reddy and Joshi [7]. On the other hand, the investigations for structured packing were also popular, and the flow and heat transfer characteristics were found to be quite different. Susskind and Becker [8] have experimentally measured the pressure drops of water in an ordered packed bed of stainless steel ball bearings. It was found that, as the relative horizontal spacing of balls increased, the pressure drop in the packed bed would be greatly decreased. Nakayama et al. [9] have numerically studied the flow in a three-dimensional spatially periodic array of cubic blocks. It was discovered that, the macroscopic hydrodynamic correlation obtained by their model could fit well with that of Ergun's equation [2], but the inertia coefficient was much lower. Calis et al. [10] and Romkes et al. [11] have investigated the flow and heat transfer characteristics in a variety of composite structured packed beds of spheres. It was revealed that, the flow and heat transfer performances in the composite structured packed beds were significantly affected by the packing form. With composite structured packings, the pressure drop could be greatly lowered and the traditional correlations (Ergun' equation [2] and Wakao's equation [5]) were unavailable for structured packings. Furthermore, the local flow distributions at the pore scale of an ordered packed bed with single phase flow were also measured by Lee and Lee [12] and Dumas et al. [13]. The detail velocity fields in the packed bed were obtained with PIV [12] and tri-segmented microelectrodes techniques [13], respectively. It was found that, the local flow distributions inside packed bed were closely related to the internal pore structures.

All these studies demonstrate that, not only local behavior but also macroscopic characteristics of flow and heat transfer are significantly affected by the internal structural properties of packed beds. The pressure drops can be greatly reduced by using structured packings and the traditional correlations are questionable for formulating flow and heat transfer performances in structured packed beds. Therefore, we can believe that, with proper selection of packing form and particle shape, the overall heat transfer performances of packed beds would be improved. In order to give a comprehensive understanding of the transport processes in structured packed beds and optimize the overall heat transfer performances, some of our recent contributions on the hydrodynamic and heat transfer characteristics in structured packed beds [14, 15] are introduced here, where the packings of ellipsoidal or non-uniform spherical particles were only investigated by our group (the Group of Novel Heat Transfer Technologies and Compact Heat Exchanger of Xi'an Jiaotong University) and some new transport phenomena were obtained.

NUMERICAL SIMULATION
Physical Model and Computational Method

The numerical simulations of flow and heat transfer process inside small pores of some novel structured packed beds with different packing forms and particle shapes were performed by Yang et al. [14].
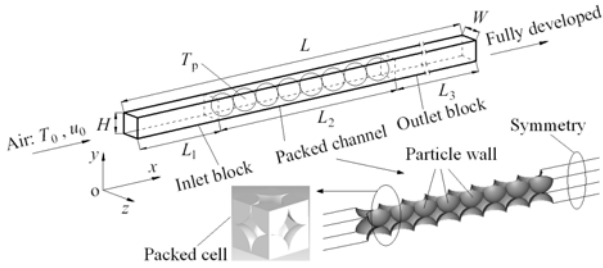
As shown in Figure 1 (a), the packed bed consisting of large number of particles (more than 1000) is orderly stacked in a square channel, where the ratio of channel height to particle diameter (N) is larger than 10. The channel walls are adiabatic and the temperature of particle surfaces is kept at T_p. Air is used as the cold fluid and the inlet temperature and velocity are kept at T_0 and u_0 respectively. For current computation condition, direct simulation of flow and heat transfer for the entire packed bed with so large number of particles is still infeasible. Therefore, representative packed channel with appropriate boundary conditions is selected for present study (see Figure 1(b)). The computational domain consists of inlet block, packed channel and outlet block. The packed channel is composed of 8 packed cells to guarantee periodically developed flow and heat transfer inside. The symmetry boundary conditions are adopted for top, bottom and side walls and the outlet flow and heat transfer are considered to be fully developed. As shown in Figure 2, six different kinds of packed cells, including three kinds of packing forms (simple cubic, body center cubic and face center cubic packings) and three kinds of particle shapes (spherical, flat ellipsoidal and long ellipsoidal particles), are selected for investigating the effects of configuration. The body center packing is divided into uniform and non-uniform packings. The non-uniform body center packing is composed of eight big particles at eight corners and one small particle at body center, where eight big particles contact with each other and the small particle contacts with all big particles. The physical dimensions of computational domain and different packed cells are presented in Table 1.

Table 1 Geometry parameters for physical models (Simulation)

Packing model	a [mm]	b [mm]	c [mm]	L_1 [mm]	L_2 [mm]	L_3 [mm]	ϕ	d_p [mm]	d_h [mm]
SC (Sphere)	12.12	12.12	12.12	30	96.96	80	0.492	12.00	7.75
BCC (Uniform sphere)	14.00	14.00	14.00	30	123.96	80	0.340	12.00	4.12
BCC-1 (Non-uniform sphere)	12.12	12.12	12.12	30	108.96	80	0.293	10.64	3.00
FCC (Sphere)	17.14	17.14	17.14	30	149.12	80	0.282	12.00	3.14
FCC-1 (Flat ellipsoid)	21.58	21.58	10.79	30	187.73	80	0.281	12.00	2.86
FCC-2 (Long ellipsoid)	27.21	13.61	13.61	30	236.72	80	0.282	12.00	2.92
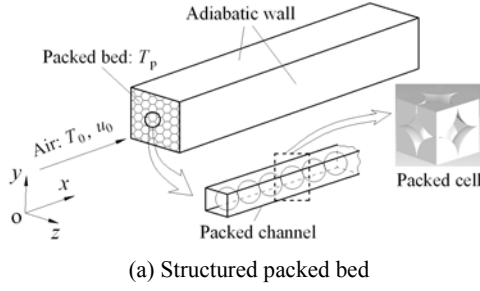
(a) Structured packed bed

(b) Representative computational domain

Figure 1 Physical model for simulation

(a) SC (Sphere) (b) BCC (Uniform sphere)

(c) BCC-1 (Non-uniform sphere) (d) FCC (Sphere)

(e) FCC-1 (Flat ellipsoid) (f) FCC-2 (Long ellipsoid)
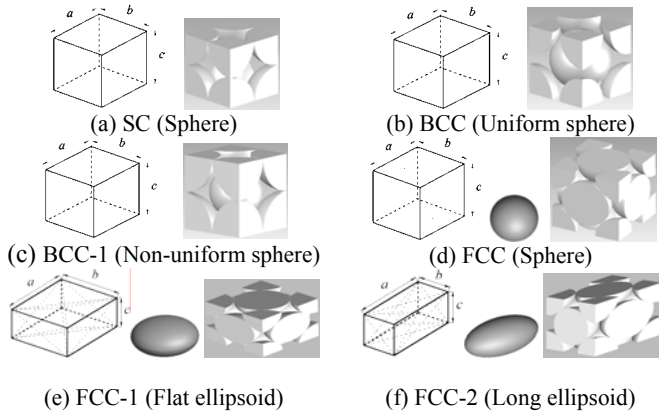
Figure 2 Different packed cells for simulation

The flow in the computational domain is considered to be incompressible and steady. Three-dimensional Navier-Stokes and energy equations are employed for the computation. The RNG k-ε turbulence model and scalable wall function are adopted for internal turbulent flow when $Re>300$. Because the computational domain is symmetrical according to y and z axis, only 1/4 part of the computational domain is finally used for the simulation. The governing equations are solved with commerc-

ial code CFX10 and the convective term in momentum equations is discretized with high resolution scheme. The continuity and momentum equations are solved together with coupled algorithm based on finite control volume method. For convergence criteria, the relative variations of the temperature and velocity between two successive iterations are demanded to be smaller than the previously specified accuracy levels of 1.0×10^{-6}. In order to avoid generating poor quality meshes at contact points between particles, the particles are stacked with very small gaps (1% of d_p) instead of contact points between each other (see Figure 3). The governing equations, boundary conditions, grid independence test and model validation are carefully formulated in Reference [14], respectively.
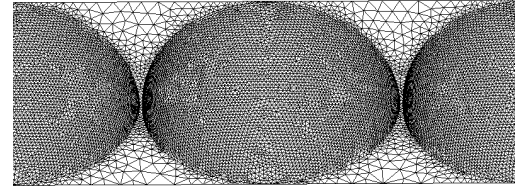

Figure 3 Part of computation grid for SC (Sphere) packing model

Basic Hydrodynamic and Heat Transfer Correlations

The macroscopic hydrodynamic and heat transfer performances in packed beds are usually formulated with traditional correlations as follows [2, 5]:

$$\frac{\Delta p}{\Delta x} = f \cdot \frac{1}{2}\rho_f\left(\frac{\left|\vec{V}_D\right|}{\phi}\right)^2 \frac{1}{d_h} \quad \left(f = \frac{c_1}{Re} + c_2\right) \quad (1)$$

$$Nu_{sf} = \frac{h_{sf} \cdot d_P}{k_f} = a_1 + a_2 Pr^{1/3} \cdot Re^n \cdot \left(\frac{d_P}{d_h}\phi\right)^n \quad (2)$$

where f is the friction factor. c_1, c_2 are the model constants in friction factor correlation, with c_1=133 and c_2=2.33 in Ergun's equation [2]. h_{sf} is the area heat transfer coefficient of particle to fluid. a_1, a_2 and n are the model constants in heat transfer equation, with a_1=2.0, a_2=1.1 and n=0.6 in Wakao's equation [5]. The Reynolds number (Re), pore scale hydraulic diameter (d_h) and equivalent particle diameter (d_p) are defined as follows:

$$Re = \frac{\rho_f\left(\left|\vec{V}_D\right|/\phi\right)d_h}{\mu_f}; \quad d_h = 4\frac{\phi}{1-\phi}\cdot\left(\frac{V_p}{A_p}\right)_{cell}; \quad d_p = 2\cdot\left(\frac{3V_p}{4\pi}\right)^{1/3} \quad (3)$$

where $\vec{V}_D$ is the Darcy velocity vector. ϕ is the porosity. V_p is the particle volume. A_p is the area of particle surface. The subscript "cell" means the value is obtained within packed cell.

Furthermore, the flow in packed beds can also be considered as flow in porous media, the macroscopic

hydrodynamics can be modeled by Forchheimer extended Darcy model [16] as follows:

$$-\frac{dp}{dx}=\frac{\mu_f}{K}\vec{V}_D+\rho_f\frac{c_F}{\sqrt{K}}\left|\vec{V}_D\right|\vec{V}_D \tag{4}$$

Compare Equation (1) with Equation (4), the permeability (K) and the Forchheimer coefficient (c_F) can be defined as follows:

$$K=\frac{d_h^2\cdot\phi}{c_1/2};\quad c_F=\frac{c_2/2}{\sqrt{c_1/2\cdot\phi^{3/2}}} \tag{5}$$

In the present study, the microscopic results obtained in the 5th to 7th packed cells are integrated and averaged to extract the macroscopic results, where the periodic flow and heat transfer are formed inside. The macroscopic pressure drop ($\Delta p/\Delta x$), heat transfer coefficient (h_{sf}) and overall heat transfer efficiency (γ) are defined as follows:

$$\frac{\Delta p}{\Delta x}=\frac{1}{3}\sum_{cell\,5}^{cell\,7}\frac{1}{(x_{out}-x_{in})A_{in}}\iint_{A_{in}}(p_{in}-p_{out})dA;$$

$$h_{sf}=\frac{1}{3}\sum_{cell\,5}^{cell\,7}\frac{\rho_f c_p\iint_{A_{in}}u(T_{f,out}-T_{f,in})dA}{A_p(T_p-\bar{T}_f)};\quad \gamma=\frac{h_{sf}}{\Delta p} \tag{6}$$

where $\bar{T}_f$ is the average temperature of fluid in packed cell. The subscript "in" and "out" mean the inlet and outlet sections of packed cell respectively.

EXPERIMENTAL STUDY
Experimental Setup and Procedure

The macroscopic hydrodynamic and heat transfer performances in the similar structured packed beds with different packing forms and particle shapes were performed by Yang et al. [15] later.

The experimental system for investigation of macroscopic hydrodynamic and heat transfer performances in the structured packed beds is shown in Figure 4. It consists of an airflow circuit, a test section and several instruments. In present study, air is induced to the wind tunnel by a centrifugal suction blower and the inlet temperature is read by a thermometer with precision of ±0.1 [ºC]. Before entering the test packed bed, the airflow is heated by passing through a removable electric heater (0-6 [kW]) and then transverses the test packed bed, where the particles inside are heated by the hot air (T_f≤85 [℃]). After the packed bed temperature increases to 70℃, the electric heater is turned off and moved away. When the packed bed temperature is stabilized (60-65 [℃]), the cold air is sucked into the channel and the packed bed is cooled down until its temperature decreases to the ambient temperature (25-28 [℃]). During the cooling process, the experimental data are measured and recorded simultaneously. The volumetric flow rate through the test section is measured by a parallel flow meter system, which is situated at the downstream of the test section. This flow meter system is composed of three different rotameters (LZB-25: 2.78×10^{-4} - 2.78×10^{-3} [m^3/s], LZB-40: 1.67×10^{-3} - 1.67×10^{-2} [m^3/s] and LZB-80: 1.39×10^{-2} - 6.94×10^{-2} [m^3/s]) and their precisions are ±5%, ±2.5% and ±4%, respectively. The static pressure difference across the test section is displayed by a micro-differential meter (Dywer-Ms-111-LCD: 0-1000 [Pa])

combined with a U-tube water column manometer (0-11760 [Pa]), whose precisions are both ±1%. The airflow and particle temperatures are measured by copper-constantan thermocouples with precision of ±0.1 [ºC] and the transient temperature signals are transformed and recorded by a real-time hybrid recorder (Keithley-2700) with a sample rate of 100 [Hz].
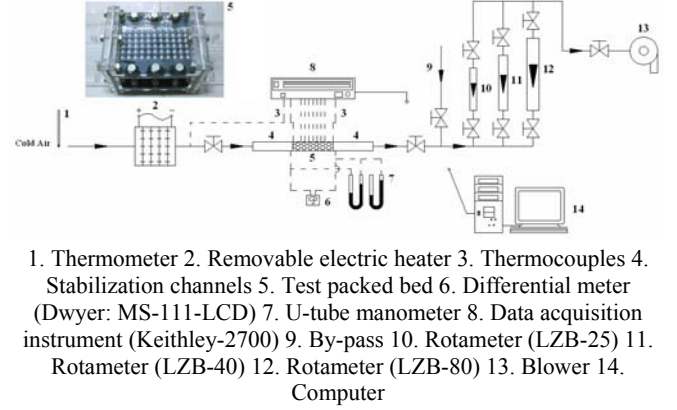

1. Thermometer 2. Removable electric heater 3. Thermocouples 4. Stabilization channels 5. Test packed bed 6. Differential meter (Dwyer: MS-111-LCD) 7. U-tube manometer 8. Data acquisition instrument (Keithley-2700) 9. By-pass 10. Rotameter (LZB-25) 11. Rotameter (LZB-40) 12. Rotameter (LZB-80) 13. Blower 14. Computer

Figure 4 Experimental system

As shown in Figure 5, the test channel is made of Plexiglas plates (thickness of 10 mm) and the particles are orderly stacked inside. In present study, the test packed bed is composed of 10(x)×5(y)×5(z) packed cells, which would guarantee the fully developed flow and heat transfer inside. Continued with numerical study of Yang et al. [14], similar structured packings are constructed, including SC (simple cubic packing with uniform spherical particles), SC-1 (simple cubic packing with uniform long ellipsoidal particles), BCC (body center cubic packing with uniform spherical particles), BCC-1 (body center cubic packing with non-uniform spherical particles) and FCC (face center cubic packing with uniform spherical particles) packings. Due to the manufacture and construction difficulties, the FCC packings of ellipsoidal particles (FCC-1 and FCC-2) for simulation [14] were not experimentally studied here. Instead, the SC packings of long ellipsoidal particles (SC-1) were constructed. Meanwhile, in order to reduce the wall effect as possible, the airflow and particle temperatures in the packed bed are only measured for the central packed channel, where the average inlet and outlet airflow temperatures are gauged by using two thermocouple
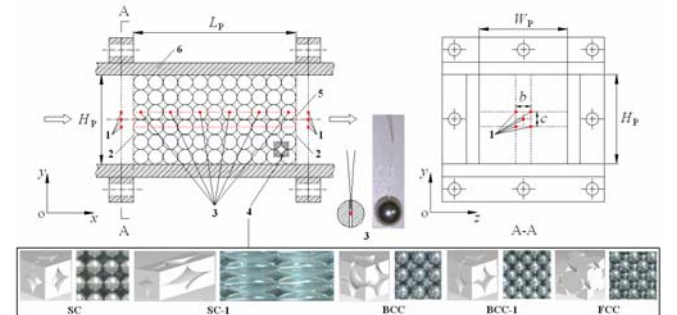

1. Thermocouples rack 2. Wire fence 3. Particle with thermocouple 4. Packed cell 5. Central packed channel 6. Plexiglas plate

Figure 5 Test packed bed

Table 2 Geometric parameters for the test packed beds (Experiment)

Packing model	a [mm]	b [mm]	c [mm]	L_p [mm]	W_p [mm]	H_p [mm]	ϕ	d_p [mm]	d_h [mm]
SC (Uniform sphere)	12.00	12.00	12.00	132.00	72.00	72.00	0.477	12.00	7.30
SC-1 (Uniform long ellipsoid)	39.10	11.72	11.72	430.10	70.32	70.32	0.477	17.51	8.78
BCC(Uniform sphere)	13.86	13.86	13.86	150.60	83.16	71.16	0.321	12.00	3.78
BCC-1 (Non-uniform Sphere)	12.12	12.12	12.12	133.20	72.72	60.72	0.278	10.71	2.80
FCC (Uniform sphere)	16.97	16.97	16.97	181.70	96.85	84.85	0.260	12.00	2.81

racks (each rack with five beads) and the particle temperatures are monitored with the thermocouples embedded in the selected particles (each particle with one bead inside). The geometric parameters and particle properties for the test packed beds are presented in Tables 2 and 3, respectively.

In present study, since accurate measurement of temperature difference between airflow and solid particles is quite difficult, it is hard to directly measure the interstitial heat transfer coefficient (h_{sf}) in the packed bed. Therefore, an inverse method of transient single-blow technique is finally used, which is considered to be suitable and convenient for determining the interstitial heat transfer coefficients in porous media. The inverse method of transient single-blow technique for present experiment is well formulated in Reference [15].

Table 3 Particle properties for the test packed beds (Experiment)

Particle shape	Material	ρ [kg/m^3]	c_p [J/kg K]	K [W/m K]
Spherical particle	Glass	2500	750.9	0.68
Long ellipsoidal particle	Bearing steel (GCr15)	7810	553.0	40.1

Data Reduction

Similar to the numerical simulations, the Nusselt number of particle to fluid (Nu_{sf}) in the test packed bed is calculated with Equation (2). The pressure drop ($\Delta p / \Delta x$), friction factor (f) and overall heat transfer efficiency (γ') in the test packed bed are defined as follows:

$$\frac{\Delta p}{\Delta x} = \frac{\Delta p_{exp}}{L_p}; \qquad f = \frac{2(\Delta p_{exp} / L_p)}{\rho_f (|\vec{V}_D| / \phi)^2 / d_h}; \qquad \gamma' = \frac{h_{sf}}{\Delta p_{exp} / L_p} \qquad (7)$$

where Δp_{exp} is the total static pressure difference across the test packed bed. L_p is the total length of the test packed bed.

According the uncertainty estimation method of Kline and McClintock [17], the maximal uncertainty of the friction factor and Nusselt number are 5.2% and 10.6%, respectively.

RESULTS AND DISCUSSION
The Effect of Packing Form

Firstly, the effect of packing form is examined. Three different kinds of packing forms are studied in this section (SC, BCC and FCC packings with uniform spheres, see Figures 2 (a), 2 (b) and 2(d) for simulation and Figure 5 for experiment).
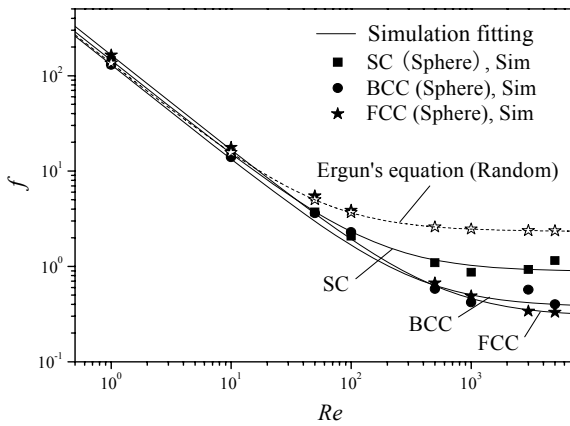
The variations of pressure drops ($\Delta p / \Delta x$) and friction factors (f) for different packing forms with simulation and experiment are presented in Figures 6 and 7, respectively. In Figures 6 (a) and 7 (a), it shows that, as Re increases, the pressure drops of different packings increase. The pressure drop

of FCC packing is the highest and it is the lowest in SC packing. In FCC packing, the porosity is the lowest and the airflow velocity inside would the highest, which will lead to the highest pressure drop inside. Furthermore, when the Reynolds number is relatively high ($Re > 100$), the inertia effect is significant and the Ergun's equation (random packing) is found to overpredict the pressure drops for structured packings. This indicates that, the hydrodynamic characteristics of structured and random packings are quite different. The tortuosities in structured packings are much lower and the pressure drops would be greatly reduced. In Figures 6 (b) and 7(b), it shows that, as Re increases, the friction factors decrease first and then keep constant ($Re > 3000$). The friction factor of SC packing is found to be higher than those of BCC and FCC packings. In SC packing, the porosity is higher. Large airflow channeling and vortices would be formed, which will lead to higher local tortuosity and friction factor inside. The model constants c_1, c_2 in friction factor correlation (in Equation (1)) are obtained by using nonlinear fitting method and the average fitting deviation is less than 10% for both simulation and experiment. The values of c_1, c_2 for different packing forms are listed in Table 4, where the results of References [2, 18] are also presented. It shows that, for structured packings, the values of c_1 are close to that in Ergun's equation (random packing), while the values of c_2 are much lower. This means, the viscosity effect (represented by c_1) in the packed bed is not so sensitive to the effect of packing form, while the inertial effect (represented by c_2) is quite different. The inertial effect in structured packing is much lower. Furthermore, due to the higher tortuosity inside, the value of c_2 for SC packing is found to be higher than those for BCC and FCC packings. In addition, it is observed that, for SC packing, the simulation results can agree well with experimental results and those reported by Martin et al. [18]. While for BCC and FCC packings, the values of c_2 with simulation are found to be lower than those of experiment. During the computational process, in order to avoid generating poor quality meshes at contact points between particles, the particles in the packed beds were assumed to be stacked with small gaps (1% of particle diameter). For SC packing, the porosity is relatively high. Large straight airflow channelling would be formed inside and the effect caused by the small gaps to the fluid flow would be small. While for BCC and FCC packings, the porosity is much lower. The airflow channelling inside is smaller and flexuous. Therefore, the effect caused by the small gaps would be larger.

The variations of Nusselt numbers (Nu_{sf}) and overall heat transfer efficiencies (γ) of particle to fluid for different packing forms with simulation and experiment are presented in Figures 8 and 9, respectively. In Figures 8 (a) and 9 (a), it shows that, as Re increases, the Nusselt numbers of different packings incr-
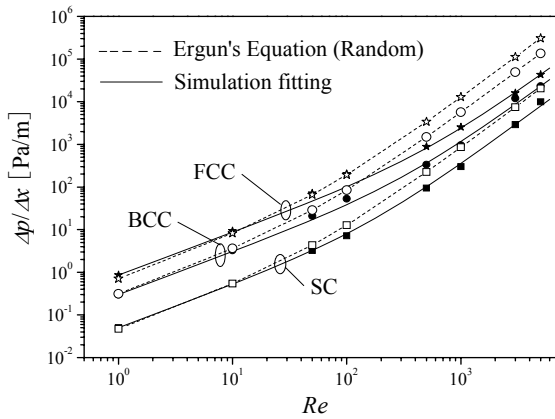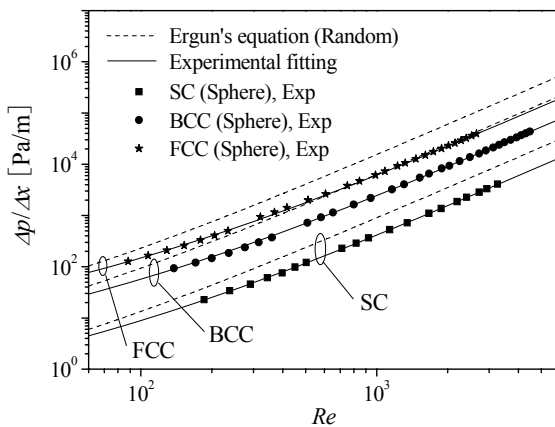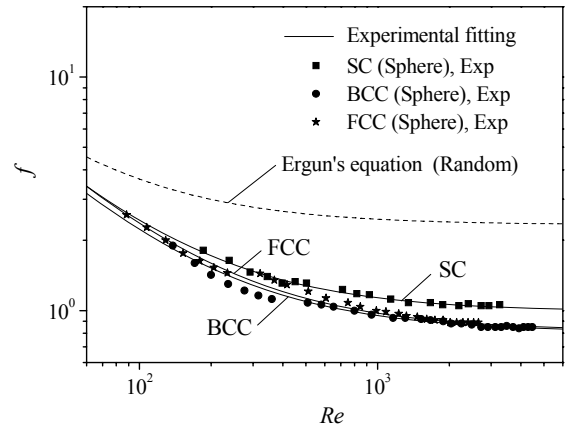
(a) $\Delta p/\Delta x$ [Pa/m]

(b) f

Figure 6 Variations of pressure drops and friction factors for different packing forms (Sphere, Simulation)

ease. The value of Nu_{sf} for FCC packing is the highest and it is the lowest for SC packing. In FCC packing, its internal structure is the most compact and the surface area-to-volume ratio is the highest, which would lead to the highest heat transfer capacity inside. Furthermore, the Wakao's equation (random packing) is found to overpredict the Nusselt numbers

(a) $\Delta p/\Delta x$ [Pa/m]

(b) f

Figure 7 Variations of pressure drops and friction factors for different packing forms (Sphere, Experiment)

Table 4 Predicted and measured values of c_1, c_2 (Sphere)

Packing model	ϕ	d_h [mm]	c_1	c_2
SC (Sphere, Simulation)	0.492	7.75	143.88	0.88
SC (Sphere, Experiment)	0.477	7.30	145.30	0.99
SC (Sphere, [18])	0.477	7.30	139.21	0.80
BCC (Sphere, Simulation)	0.340	4.12	129.81	0.37
BCC (Sphere, Experiment)	0.321	3.78	142.25	0.81
FCC (Sphere, Simulation)	0.282	3.14	164.12	0.30
FCC (Sphere, Experiment)	0.260	2.81	155.00	0.82
Random (Ergun' equation [2])	/	/	133.00	2.33

for structured packings. The model constants a_1, a_2 and n in heat transfer correlation (in Equation (2)) for present study are obtained by using nonlinear fitting method and the average fitting deviation is less than 10% for both simulation and experiment. The values of a_1, a_2 and n for different packing forms are listed in Table 5. It shows that, for structured packings, the values of a_1 and n are close to those in Wakao's equation (random packing), while the values of a_2 are much lower. In addition, it is discovered that, for different structured packings, the simulation results can agree well with those of experiments, which is quite different to the case presented in Table 4. In the experiment, the particles are stacked with points. The conduction effects between particles are quite small and the heat transfer in the packed bed is mainly affected by the effects of internal convections. During numerical simulations, the particles in the packed beds were assumed to be stacked with small gaps. The corresponding variation caused by the conductions between particles is insignificant and the total heat transfer in the packed bed is almost unchanged. Therefore, the numerical and experimental results can agree well with each other. In Figures 8 (b) and 9 (b), it shows that, as Re increases,
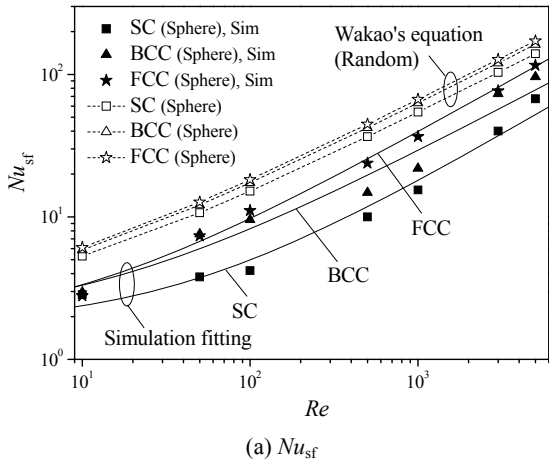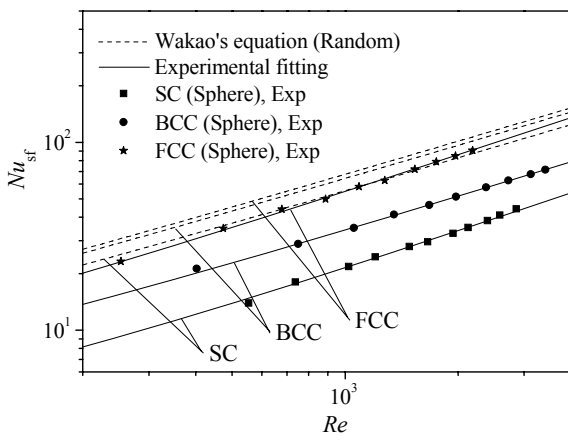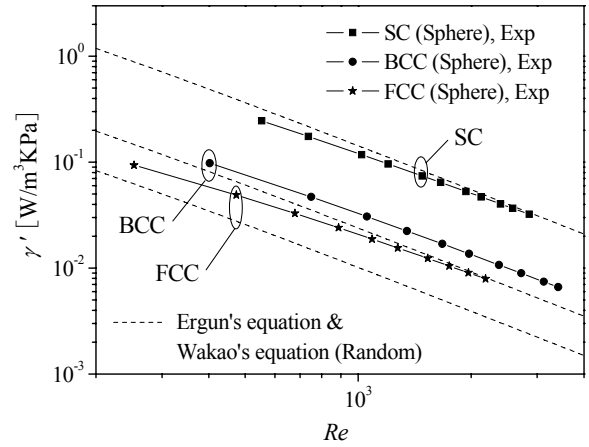
(a) Nu_{sf}
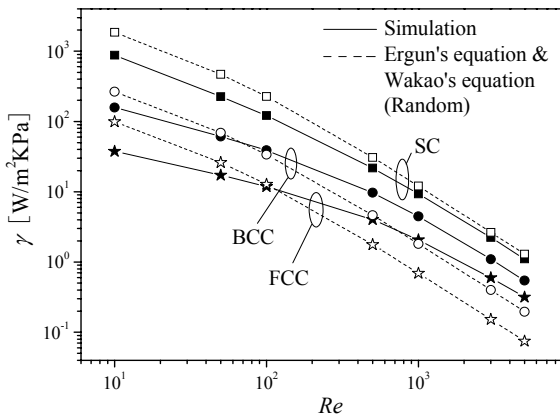
(b) γ [W/m²KPa]

Figure 8 Variations of Nusselt numbers and overall heat transfer efficiencies of particle to fluid for different packing forms (Sphere, Simulation)

the overall heat transfer efficiencies of different packings decreases. The value of γ for SC packing is the highest and it is the lowest for FCC packing, which indicates that, high heat transfer performance of FCC packing is obtained at cost of high

(a) Nu_{sf}

(b) γ' [W/m³KPa]

Figure 9 Variations of Nusselt numbers and overall heat transfer efficiencies of particle to fluid for different packing forms (Sphere, Experiment)

Table 5 Predicted and measured values of a_1, a_2 and n (Sphere)

Packing model	ϕ	d_h [mm]	d_p [mm]	a_1	a_2	n
SC (Sphere, Simulation)	0.492	7.75	12.00	1.73	0.16	0.7
SC (Sphere, Experiment)	0.477	7.30	12.00	1.73	0.20	0.7
BCC (Sphere, Simulation)	0.340	4.12	12.00	1.8	0.4	0.63
BCC (Sphere, Experiment)	0.321	3.78	12.00	2.1	0.46	0.63
FCC (Sphere, Simulation)	0.282	3.14	12.00	1.6	0.41	0.67
FCC (Sphere, Experiment)	0.260	2.81	12.00	2.2	0.54	0.67
Random (Wakao' equation [5])	/	/	/	2.0	1.1	0.6

pressure drop, and its overall heat transfer performance is relatively low. Furthermore, it is found that, with the same physical parameters, the overall heat transfer efficiency of SC packing is lower than that of random packing, while for BCC and FCC packings, the overall heat transfer efficiencies are much higher. This indicates that, the hydrodynamic and heat transfer characteristics of structured and random packings are quite different. With proper selection of packing form (such as BCC and FCC packings), the overall heat transfer performance will be improved.
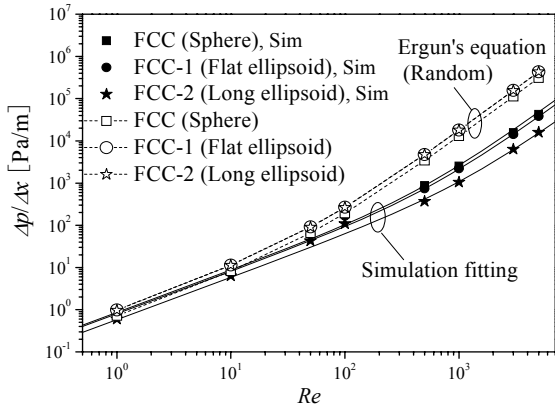
The Effect of Particle Shape

In this section, the effect of particle shape is investigated. Three different kinds of particles are compared for the simulation, including spherical (FCC, see Figure 2 (d)), flat ellipsoidal (FCC-1, see Figure 2 (e)) and long ellipsoidal particles (FCC-2, see Figure 2 (d)). Due to the manufacture and construction difficulties, the FCC packings of different particles were not experimentally studied here. Instead, the SC packings
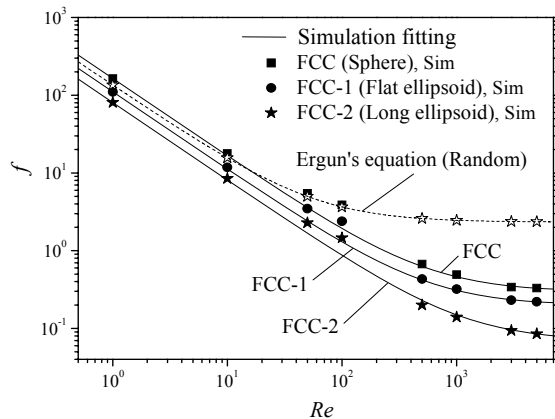
were adopted, including SC (Spherical particle) and SC-1 (Long ellipsoidal particle) packings (see Figure 5).

The variations of pressure drops ($\Delta p/\Delta x$) and friction factors (f) for different particle models with simulation (FCC) and experiment (SC) are presented in Figures 10 and 11, respectively. It shows that, under the same Reynolds number, the pressure drop and friction factor of ellipsoidal particle models (FCC-1, FCC-2 and SC-1) are much lower than those of spherical particle model (FCC and SC) and the Ergun's equation (random packing) is found to overpredict the pressure drops and friction factors for different particle models. In FCC-1, FCC-2 and SC-1 packings, with better hydraulic particle shape (ellipsoid), the local airflow velocity and tortuosity would be much lower, which would lead to lower pressure drop and friction factor inside. This indicates that, under the same packing form, the pressure drop and friction fiction factor in the packed bed will be further reduced with proper selection of particle shapes. The friction factor constants c_1, c_2 for different particle models are obtained by using nonlinear fitting method and the average fitting deviation is less than 10% for both simulation and experiment. The values of c_1, c_2 for different particle models with simulation (FCC) and experiment (SC) are presented in Tables 6 and 7, respectively. It shows that, for different particle models, the values of c_1 are close to that in

Ergun's equation (random packing), while the values of c_2 are much lower. Furthermore, due to the lower tortuosity inside, the value of c_2 for ellipsoidal particle models (FCC-1, FCC-2 and SC-1) is found to be much lower than that for spherical particle models (FCC and SC).
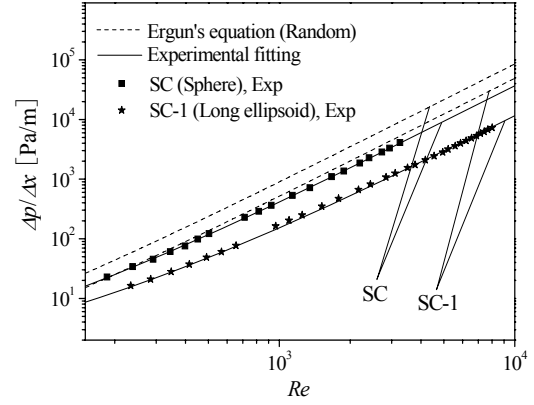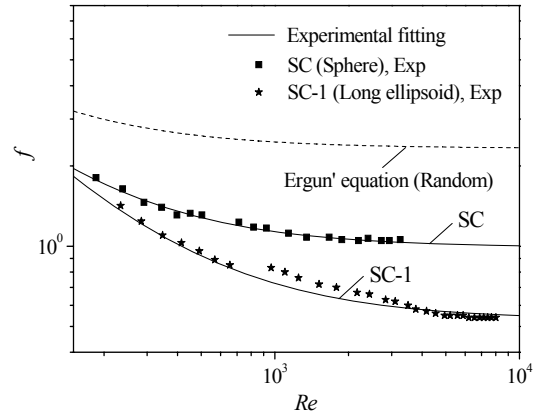

(a) $\Delta p/\Delta x$ [Pa/m]

(b) f

Figure 11 Variations of pressure drops and friction factors for SC packings with different particles (Experiment)

Table 6 Predicted values of c_1, c_2 (FCC)

Packing model	ϕ	d_h [mm]	c_1	c_2
FCC (Sphere, Simulation)	0.282	3.136	164.12	0.297
FCC-1 (Flat ellipsoid, Simulation)	0.281	2.855	110.43	0.198
FCC-2 (Long ellipsoid, Simulation)	0.282	2.915	80.35	0.069
Random (Ergun' equation [2])	/	/	133	2.33

Table 7 Measured values of c_1, c_2 (SC)

Packing model	ϕ	d_h [mm]	c_1	c_2
SC (Sphere, Experiment)	0.477	7.30	145.30	0.99
SC-1 (Long ellipsoid, Experiment)	0.477	8.78	195.00	0.53
Random (Ergun' equation [2])	/	/	133.00	2.33

(a) $\Delta p/\Delta x$ [Pa/m]

(b) f

Figure 10 Variations of pressure drops and friction factors for FCC packings with different particles (Simulation)

The variations of Nusselt numbers (Nu_{sf}) and overall heat transfer efficiencies (γ) of particle to fluid for different particle models with simulation (FCC) and experiment (SC) are

presented in Figures 12 and 13, respectively. It shows that, the Nusselt numbers of different particle models are close to each other and the Wakao's equation (random packing) is found to overpredict the Nusselt numbers for different particle models. The heat transfer constants a_1, a_2 and n for different particle models are obtained by using nonlinear fitting method and the average fitting deviation is less than 10% for both simulation and experiment. The values of a_1, a_2 and n for different particle models with simulation (FCC) and experiment (SC) are presented in Tables 8 and 9, respectively. It shows that, for different particle models, the values of a_1 and n are close to those in Wakao's equation (random packing), while the values of a_2 are much lower. In Fig. 9 (b), it shows that, as Re increases, the overall heat transfer efficiencies of different particle models decrease. With the same physical parameters, the overall heat transfer efficiency of ellipsoidal particle models (FCC-1, FCC-2 and SC-1) is much higher than that of random packing and it is also higher than that of spherical particle models (FCC and SC). This indicates that, for different particle models, the hydrodynamic and heat transfer characteristics of structured packings are different. Under the same packing form, the overall heat transfer performance will be further improved with proper selection of particle shape (such as ellipsoidal particle).
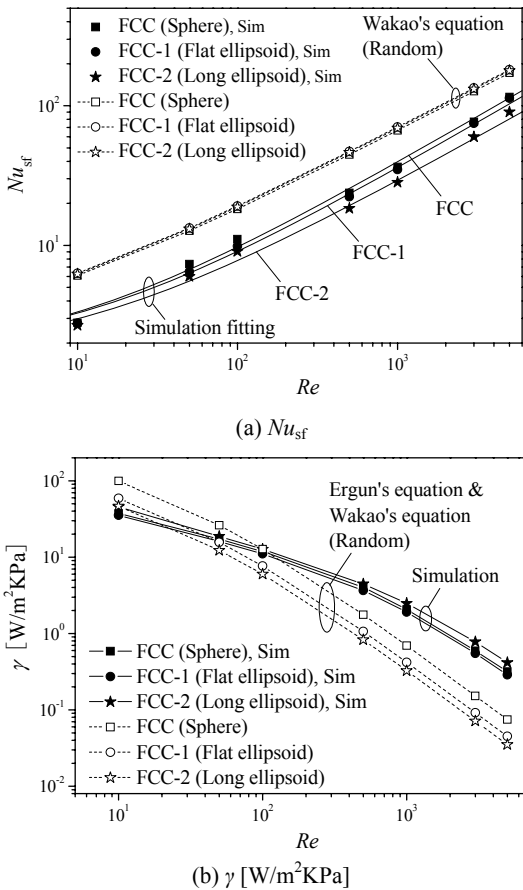

(a) Nu_{sf}

(b) γ [W/m^{2}KPa]

Figure 12 Variations of Nusselt numbers and overall heat transfer efficiencies of particle to fluid for FCC packings with different particles (Simulation)
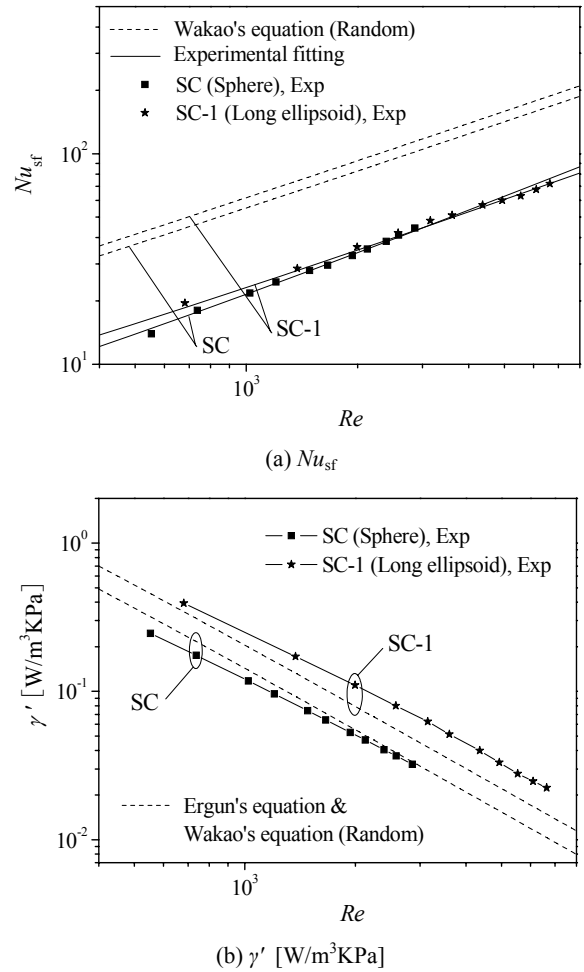

(a) Nu_{sf}

(b) γ' [W/m^{3}KPa]

Figure 13 Variations of Nusselt numbers and overall heat transfer efficiencies of particle to fluid for SC packings with different particles (Experiment)

Table 8 Predicted values of a_1, a_2 and n (FCC)

Packing model	ϕ	d_h [mm]	d_p [mm]	a_1	a_2	n
FCC (Sphere, Simulation)	0.282	3.136	12.00	1.60	0.40	0.67
FCC-1 (Flat ellipsoid, simulation)	0.281	2.855	12.00	1.70	0.34	0.67
FCC-2 (Long ellipsoid, simulation)	0.282	2.915	12.00	1.60	0.32	0.65
Random (wakao' equation [5])	/	/	/	2.00	1.10	0.60

Table 9 Measured values of a_1, a_2 and n (SC)

Packing model	ϕ	d_h [mm]	d_p [mm]	a_1	a_2	n
SC (Sphere, Experiment)	0.477	7.30	12.00	1.73	0.20	0.7
SC-1 (Long ellipsoid, Experiment)	0.477	8.78	17.51	1.8	0.32	0.63
Random (Wakao' equation [5])	/	/	/	2.0	1.1	0.6

## Performance Comparison for U niform and N on-uniform Packings

Finally, the performances of uniform and non-uniform packings are compared. Since the non-uniform BCC packing form is stable and easy to be constructed, the BCC packing form is adopted, including BCC (Uniform sphere) and BCC-1(Non-uniform sphere) packings, see Figures 2 (b) and 2 (c) for simulation and Figure 5 for experiment).

The variations of pressure drops ($\Delta p/\Delta x$) and friction factors (f) for BCC and BCC-1 packings with simulation and experiment are presented in Figures 14 and 15, respectively. It shows that, under the same Reynolds number, the pressure drop and friction factor of BCC-1 packing are much higher than those of BCC packing and the Ergun's equation (random packing) is found to overpredict the pressure drops and friction factors for both packings. In BCC-1 packing, the porosity is much lower and the airflow velocity inside would be much higher, which would lead to the higher pressure drop inside. Furthermore, due to the non-uniformity packing characteristic inside, the tortuosity in BCC-1 packing would also be higher. However, although the pressure drop and tortuosity in non-uniform packing are much higher, they are still much lower than those in random packing. The friction factor constants c_1, c_2 for BCC and BCC-1 packings are obtained by using nonlinear fitting method and the average fitting deviation is less than 10% for both simulation and experiment. The values of c_1, c_2 for both packings are presented in Table 10. It shows that, for uniform and non-uniform packings, the values of c_1 are close to that in Ergun's equation (random packing), while the values of c_2 are much lower. Due to the higher tortuosity inside, the value of c_2 for BCC-1 packing is found to be much higher than that for BCC packing. Furthermore, the deviation of c_2 between simulation and experimental results for BCC-1 packing is also existed. The effect caused by the small gaps in the simulation is significant and the simulation is found to underestimate the friction factor in BCC-1 packing.

The variations of Nusselt numbers (Nu_{sf}) and overall heat transfer efficiencies (γ) of particle to fluid for BCC and BCC-1 packings with simulation and experiment are presented in Figures 16 and 17, respectively. In Figures 16 (a) and 17 (a), it shows that, the Nusselt number of BCC-1 packing is higher
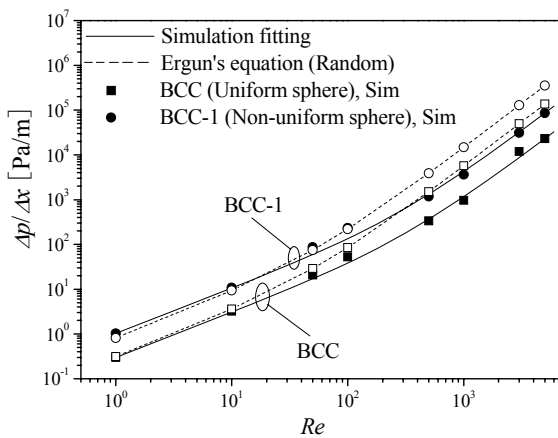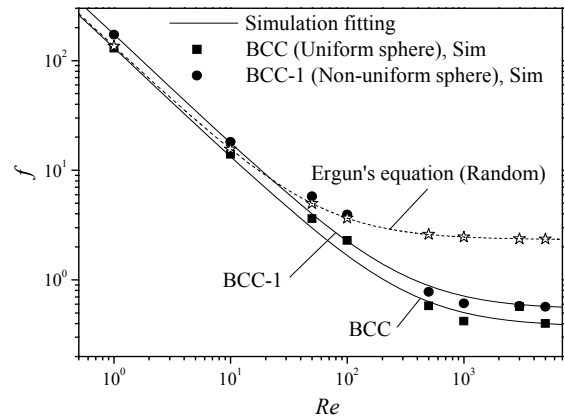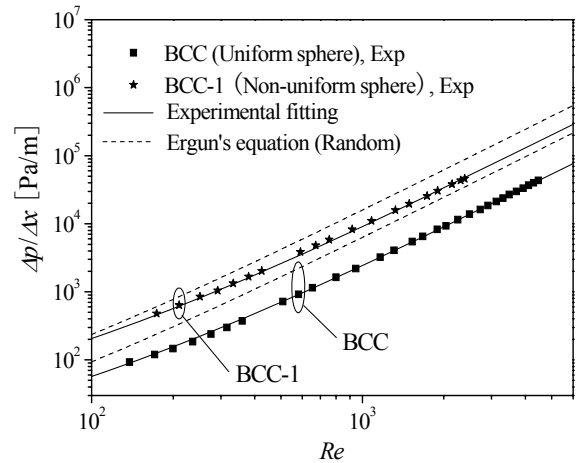
(b) f

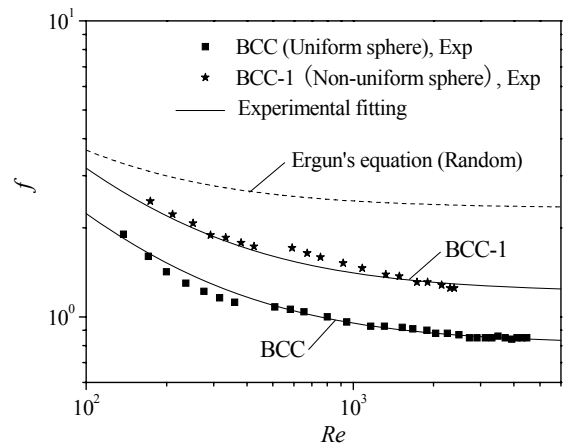**Figure 14** Variations of pressure drops and friction factors for uniform and non-uniform packings with spherical particles (Simulation)

(a) $\triangle p/\triangle x$ [Pa/m]

(b) f

Figure 15 Variations of pressure drops and friction factors for uniform and non-uniform packings with spherical particles (Experiment)
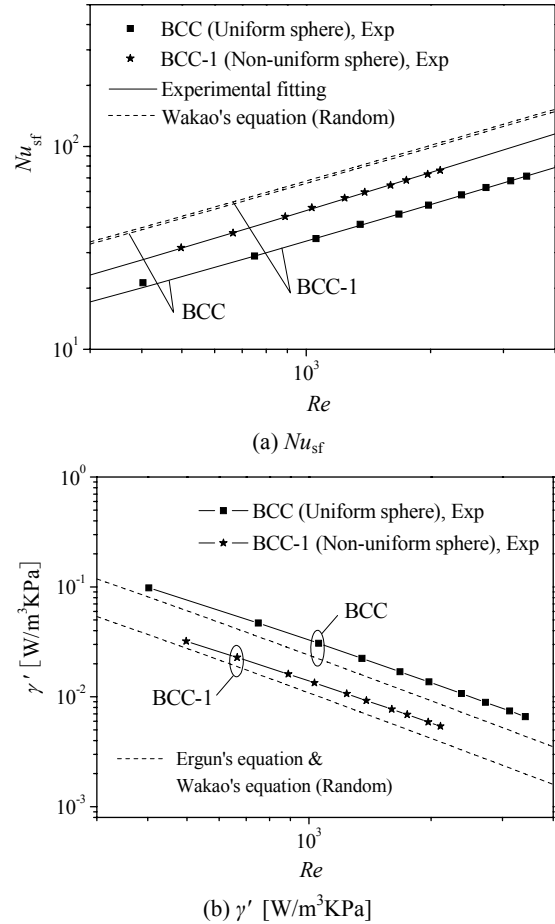
(a) $\triangle p/\triangle x$ [Pa/m]

287

Table 10 Predicted and measured values of c_1, c_2 (BCC)

Packing model	ϕ	d_h [mm]	c_1	c_2
BCC (Uniform sphere, Simulation)	0.340	4.12	129.81	0.37
BCC (Uniform sphere, Experiment)	0.321	3.78	142.25	0.81
BCC-1 (Non-uniform sphere, Simulation)	0.293	3.00	172.53	0.54
BCC-1 (Non-uniform sphere, Experiment)	0.278	2.80	197.00	1.21
Random (Ergun' equation [2])	/	/	133.00	2.33

than that of BCC packing, and the Wakao's equation (random packing) is found to overpredict the Nusselt numbers for both packings. In BCC-1 packing, its configuration is more compact and the surface area-to-volume ratio is higher, which would lead to higher heat transfer efficiency inside. The heat transfer constants a_1, a_2 and n for BCC and BCC-1 packings are obtained by using nonlinear fitting method and the average fitting deviation is less than 10% for both simulation and experiment. The values of a_1, a_2 and n for both packings are presented in Table 11. It shows that, for uniform and non-uniform packings, the values of a_1 and n are close to those in

(a) Nu_{sf}

(b) γ [W/m^{2}KPa]
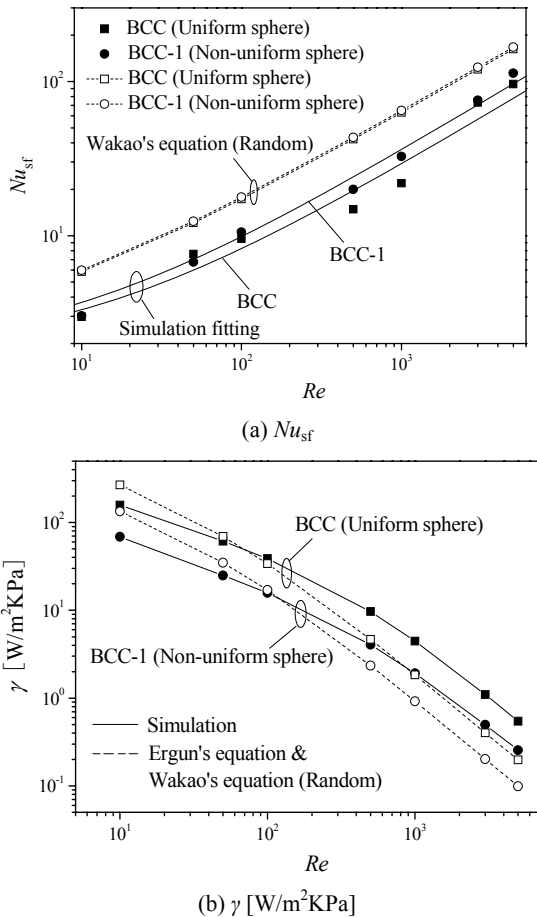
Figure 16 Variations of Nusselt numbers and overall heat transfer efficiencies of particle to fluid for uniform and non-uniform packings with spherical particles (Simulation)

Wakao's equation (random packing), while the values of a_2 are much lower. Furthermore, it is found that, for non-uniform packing, the simulation and experimental results can also agree well with each other. In Figures 16 (b) and 17 (b), it shows that, as Re increases, the overall heat transfer efficiencies for BCC and BCC-1 packings decrease. With the same physical parameters, the values of γ for both packings are much higher than those of random packings. And the overall heat transfer efficiency of BCC packing is found to be higher than that of BCC-1packing. This indicates that, under the same packing

(a) Nu_{sf}

(b) γ' [W/m^{3}KPa]

Figure 17 Variations of Nusselt numbers and overall heat transfer efficiencies of particle to fluid for uniform and non-uniform packings with spherical particles (Experiment)

Table 11 Predicted and measured values of a_1, a_2 and n (BCC)

Packing model	ϕ	d_h [mm]	d_p [mm]	a_1	a_2	n
BCC (Uniform sphere, Simulation)	0.340	4.12	12.00	1.8	0.40	0.63
BCC (Uniform sphere, Experiment)	0.321	3.78	12.00	2.1	0.46	0.63
BCC-1 (Non-uniform sphere, Simulation)	0.293	3.00	10.64	1.8	0.49	0.63
BCC-1 (Non-uniform sphere, Experiment)	0.278	2.80	10.71	2.2	0.56	0.65
Random (Wakao' equation [5])	/	/	/	2.0	1.1	0.6

form and particle shape, the heat transfer performance will be further improved with non-uniform packing method. However, due to the higher flow resistant inside, the overall heat transfer performance in non-uniform packing is lower.

CONCLUDSIONS

In present paper, some of our recent contributions on the hydrodynamic and heat transfer characteristics in some novel structured packed beds are introduced, where the packings of ellipsoidal or non-uniform spherical particles were only investigated by our group and some new transport phenomena were obtained. The effects of packing form and particle shape are carefully investigated, and the numerical and experimental results are also compared in detail. The major findings are as follows:

(1) With proper selection of packing form and particle shape, the pressure drop in structured packed beds can be greatly reduced and the overall heat transfer performance will be improved. The traditional correlations are found to overpredict the pressure drops and Nu_{sf} for all the structured packings, and the modified correlations are obtained. The forms of these new correlations can fit well with those of traditional correlations, but some model constants, such as c_2 and a_2, are much lower.

(2) In the numerical simulations, the particles in the packed beds were assumed to be stacked with small gaps (1% of particle diameter), which would be good for mesh generating between particles. This manner is proved to be suitable for heat transfer predictions in structured packings, but it is found to underestimate the friction factors, especially when the porosity is relatively low.

(3) Both the effects of packing form and particle shape are found to be significant to the macroscopic hydrodynamic and heat transfer characteristics in structured packed beds. With the same particle shape (sphere), the Nusselt number (Nu_{sf}) of FCC packing is the highest and it is the lowest for SC packing. While for SC packing, the pressure drop is the lowest and its overall heat transfer efficiency is the highest; with the same packing form (FCC or SC), the heat transfer characteristics of spherical and ellipsoidal particle models are similar, while the pressure drops of ellipsoidal particle models (FCC-1, FCC-2 and SC-1) are much lower and their overall heat transfer performances are better; furthermore, with the same packing form (BCC packing) and particle shape (sphere), the heat transfer performance in the packed bed will be further improved by using non-uniform packing method. While due to the higher flow resistant inside, the overall heat transfer efficiency in non-uniform packing (BCC-1) is lower.

ACKNOWLEDGEMENTS

REFERENCES

[1] Carpinlioglu M.O., and Ozahi E., A simplified correlation for fixed bed pressure drop, *Powder Technology*, Vol. 187, 2008, pp. 94-101.

[2] Ergun S., Fluid flow through packed columns, *Chemical Engineering Progress*, Vol. 48, 1952, pp. 89-94.

[3] Lanfrey P.Y., Kuzeljevic Z.V., and Dudukovic M.P., Tortuosity model for fixed beds randomly packed with identical particles, *Chemical Engineering Science*, Vol. 65, 2010, pp. 1891-1896.

[4] Guardo A., Coussirat M., Larrayoz M.A., Recasens F., and Egusquiza E., Influence of the turbulence model in CFD modeling of wall-to-fluid heat transfer in packed beds, *Chemical Engineering Science*, Vol. 60, 2005, pp. 1733-1742.

[5] Wakao N., and Kaguei S., Heat and mass transfer in packed beds, McGraw-Hill, New York, 1982.

[6] Guo X.Y., and Dai D., Numerical simulation of flow and heat transfer in a random packed bed, *Particuology*, Vol. 8, 2010, pp. 293-299.

[7] Reddy R.K., and Joshi J.B., CFD modeling of pressure drop and drag coefficient in fixed beds: Wall effects, *Particuology*, Vol. 8, 2010, pp. 37-43.

[8] Susskind H., and Becker W., Pressure drop in geometrically ordered packed beds of spheres, *AIChE Journal*, Vol. 13, 1967, pp. 1155-1159.

[9] Nakayama A., Kuwahara F., Kawamura Y., and Koyama Y.H., Three-dimensional numerical simulation of flow through a microscopic porous structure, *ASME/JSME Thermal Engineering Conference*, 1995, pp. 313-318.

[10] Calis H.P.A., Nijenhuis J., Paikert B.C., Dautzenberg F.M., and van den Bleek C.M., CFD modelling and experimental validation of pressure drop and flow profile in a novel structured catalytic reactor packing, *Chemical Engineering Science*, Vol. 56, 2001, pp. 1713-1720.

[11] Romkes S.J.P., Dautzenberg F.M., van den Bleek C.M., and Calis H.P.A., CFD modelling and experimental validation of particle-to-fluid mass and heat transfer in a packed bed at very low channel to particle diameter ratio, *Chemical Engineering Journal*, Vol. 96, 2003, pp. 3-13.

[12] Lee J.Y., and Lee S.Y., Flow visualization in the scaled up pebble bed of high temperature gas-cooled reactor using particle image velocimetry method, *Journal of Engineering for Gas Turbines and Power*, Vol. 131, 2009, pp. 1-4.

[13] Dumas T., Lesage F., and Latifi M.A., Modelling and measurements of the velocity gradient and local flow direction at the pore scale of a packed bed, *Chemical Engineering Research and Design*, Vol. 88, 2010, pp. 379-384.

[14] Yang J., Wang Q.W., Zeng M., and Nakayama A., Computational study of forced convective heat transfer in structured packed beds with spherical or ellipsoidal particles, *Chemical Engineering Science*, Vol. 65, 2010, pp. 726-738.

[15] Yang J., Wang J., Bu S.S., Zeng M., Wang Q.W., and Nakayama A., Experimental analysis of forced convective heat transfer in novel structured packed beds of particles, *Chemical Engineering Science*, 2011. (Submitted)

[16] Nield D.A., and Bejan A., Convection in Porous Media (third ed.), Springer, New York, 2006.

[17] Kline S.J., and McClintock F.A., Describing uncertainties in single-sample experiments, *Mechanical Engineering*, Vol. 75, 1953, pp. 3–8.

[18] Martin J.J., McCabe W.L., and Monrad C.C., Pressure drop through stacked spheres, *Chemical Engineering Progress*, Vol. 47, 1951, pp. 91–94.